4D CBCT reconstruction with TV regularization on a dynamic software phantom

Rob Heylen, Georg Schramm, Paul Suetens, Johan Nuyts

***Abstract*—In 2011 a primal-dual optimization algorithm was proposed by Chambolle and Pock. This algorithm is well fit for 4D CBCT reconstruction with spatial and temporal total variation (TV) regularization, and several authors recently used this approach. In this paper, we also implement a version of this algorithm, and assess its capabilities for dual-energy dynamic angiography of the brain on a software phantom. The phantom is created by adding an artificial vasculature, generated with constrained constructive optimization, to the Brainweb phantom, and by calculating blood flow dynamics through this vasculature based on hydrodynamic equations. A dual-energy CBCT acquisition is simulated, split into water and iodine components, and a 4D iodine image is reconstructed. This suggests the viability of 4D CBCT techniques based on TV for dual-energy dynamic brain angiography.**

I. 4D CBCT WITH TV REGULARIZATION

4D CBCT allows the reconstruction of several time frames, and can be used to visualize the flow of contrast through the brain vasculature, which has a large diagnostic potential in the acute ischemic stroke workflow. Furthermore, dual-energy (DE) CBCT devices are becoming more accessible, which significantly increases the capabilities of CBCT examination.

Many authors have shown that total variation (TV) regularization in both the time and spatial domain is very useful for 4D CBCT reconstruction, with applications in cardiac, pulmonary and brain imaging [1], [2]. Computationally efficient implementations based on the primal-dual optimization algorithm of Chambolle and Pock [3] have recently been presented by several authors [4], [5], [6].

To assess the capabilities of these types of algorithms for dual-energy dynamic angiography of the brain, we have created a software phantom that includes the flow of a bolus of contrast through a simulated vasculature. The aim is to reconstruct a dynamic iodine image.

II. THE ALGORITHM

Consider a contrast-enhanced CBCT acquisition yielding a sinogram $s = (s_{ijf}) \in S = \mathbb{R}_+^{M_1 M_2 F}$, with $1 \leq i \leq M_1$, $1 \leq j \leq M_2$ and $1 \leq f \leq F$ indexing the two spatial and the temporal (angular) directions respectively. We want to reconstruct T time frames $x = x_{ijkt} \in X = \mathbb{R}_+^{N_1 N_2 N_3 T}$, where $1 \leq i \leq N_1$, $1 \leq j \leq N_2$, $1 \leq k \leq N_3$ and $1 \leq t \leq T$ index the three spatial and the temporal directions respectively.

The data set x can be forward-projected to a sinogram with the projector $A : X \to S$, which depends on the geometrical details of the CBCT setup and the projection algorithm. The back-projection is given by the adjoint operation A^*.

The projector linearly interpolates between the time frames: Let x^t be the time frames in x, where x^1 and x^T correspond to the first and last projection in the sinogram respectively. Each projection s_f corresponds to a continuous time point $\hat{t} = 1 + (T-1)f/F \in [1, T]$, which can be decomposed into an index $I = \lfloor \hat{t} \rfloor$ and a fraction $f = \hat{t} - I$. The forward projection s_f is obtained by projecting a linearly interpolated 3D data set $(1-f)x^I + fx^{I+1}$. Backprojection can be implemented similarly, where contributions from each projection in the sinogram are properly distributed over their contributing time frames.

Furthermore, we can incorporate a binary voxel mask in the projector to indicate static voxels, i.e., voxels that should not contain any dynamics [4]. These voxels have the same value for all time frames. Masking out highly-attenuating structures that contain no contrast dynamics, such as bone, can greatly improve the performance of the algorithm.

We consider the optimization algorithm

$$\underset{x \in X}{\operatorname{argmin}} \left(\|Ax - s\|_2^2 + \alpha \|x\|_{\text{TV4}} + \mathrm{I}_{\mathbb{R}^{\mathbb{N}+}}(x) \right) \tag{1}$$

The first term promotes data consistency between the forward projection and the sinogram. The TV term is a 4D TV, and is weighted by α:

$$\|x\|_{\text{TV4}} = \sum_{ijkt} |(\Delta x)_{ijkt}| \tag{2}$$

$$|(\Delta x)_{ijkt}| \quad = \quad \left(\sum_{d=1}^{3} (\Delta_d x)_{ijkt}^2 + (\gamma \Delta_4 x)_{ijkt}^2 \right)^{1/2} \tag{3}$$

The γ factor in the last term weighs the spatial and temporal directions differently. The Δ_i operator is the forward discrete difference operator over dimension i. The adjoint is given by a weighted negative divergence.

The third term is the characteristic function of the positive orthant, and penalizes any solution with negative entries. This equation can be written in terms of the Chambolle and Pock framework, yielding algorithm 1 to solve (1). See [3], [4], [6] for more information. The projection on the set αP in line 5 projects each gradient voxel-wise onto a ball of radius α.

Note that the forward projection A and backward projection A^* are scaled such that the largest eigenvalue of A^*A equals one. This scaling constant is obtained via power iterations. Also the TV operator and its adjoint are normalized accordingly.

Manuscript received November 26, 2019.

R.H., G.S. and J.N. are with the Department of Imaging and Pathology, Division of Nuclear Medicine, KULeuven, Belgium. P.S. is with the Processing speech and images group of the Faculty of Engineering science, KULeuven, Belgium. This work was done under the NEXIS project, that has received funding from the European Union's Horizon 2020 Research and Innovations Programme (Grant Agreement #780026).

978-1-7281-4164-0/19/$31.00

Algorithm 1: The proposed algorithm

Initialize all variables, choose τ, $\sigma > 0$, $\theta \in [0, 1]$;
for $n \geq 0$ **do**
$y_1^{n+1} = \frac{2}{2+\sigma}\left(y_1^n + \sigma(A\overline{x} - s)\right)$;
$x_1^{n+1} = A^* y_1^{n+1}$;
$y_2^{n+1} = \mathrm{proj}_{\alpha P}\left(y_2^n + \sigma\Delta\overline{x}\right)$;
$x_2^{n+1} = -\mathrm{div}\left(y_2^{n+1}\right)$;
$x^{n+1} = \mathrm{proj}_{\mathbb{R}^{N+}}\left(x^n - \tau x_1^{n+1} - \tau x_2^{n+1}\right)$;
$\overline{x}^{n+1} = x^{n+1} + \theta(x^{n+1} - x^n)$;

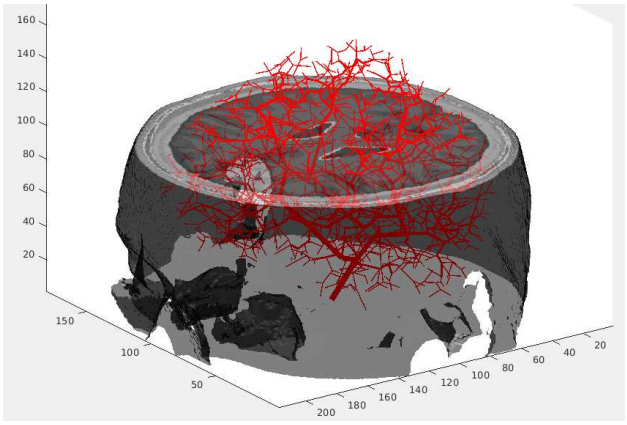

Fig. 1: The simulated vasculature inside the brainweb phantom.

III. A dynamic phantom for angiography

We created a dynamic phantom for testing the capabilities of the presented algorithm on simulated DE CBCT scans. The starting point is the brainweb phantom [7], a voxelized head phantom where 10 tissue classes are present. These classes are fuzzy, and more than one class may be present in each voxel, with the abundances summing to one over all classes.

Next, we generated an artificial vasculature by implementing the constrained constructive optimization method from [8], where the initial (root) segment was located where the carotid artery is expected, and random generation of arterial output terminals was constrained to gray/white matter tissue classes. The result is visualized in Fig. 1 for 1000 terminal points.

A contrast input function was obtained from a single voxel in the carotid area of an actual CT angiography examination. This input function was passed through the artificial vasculature, where each tube segment was considered to possess laminar flow so that dispersion and time delays can be calculated analytically [9]. The diffusion coefficient was fitted to the input data, and a realistic time behaviour of the flow of contrast is obtained. Note that no attempt was done to obtain a realistic anatomy. In addition, no draining venous network was simulated, and the contrast will disappear at the arterial output terminals of the vascular tree. We do expect this type of simulation to be adequate for assessing 4D CBCT algorithms.

The artificial vascular tree was voxelized, and added to the brainweb phantom as an additional dynamic class. For each projection in the sinogram, an appropriate time point was calculated, and the corresponding iodine contribution from the vascular tree determined. Forward projection was obtained with a dual-energy CBCT simulator. Sinogram domain decomposition was performed into a water and an iodine component via Newton optimization of the spectrum - sinogram relationship.

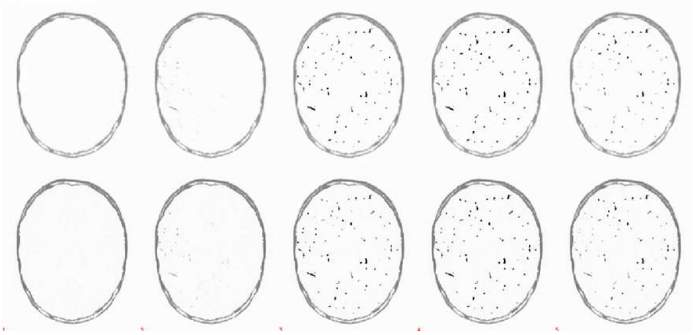

Fig. 2: Reconstruction (top) and ground truth (bottom) of 5 time frames on a synthetic data set. Axial slice, iodine component.

IV. Experiment

We have executed the algorithm on the iodine sinogram component obtained with the dynamic brainweb phantom. 200 frames of 250×250 pixels were simulated over $360°$. We reconstructed 5 time frames from this data set, where every time frame was initialized with a prior image obtained with the FDK algorithm on a non-contrast enhanced synthetic data set. The parameters were $\tau = 3.5$, $\sigma = 0.95/\tau$, $\theta = 1$, $\alpha = 1e-7$, $\gamma = 100$ and the number of iterations was 50. These values were obtained heuristically. A static bone mask was employed in the projector.

The result is shown in Fig. 2, along with the ground truth. It is clear that there is good agreement between both.

V. Conclusion and future work

The Chambolle-Pock algorithm is a powerful optimization algorithm used by several authors to derive a 4D TV regularized iterative reconstruction algorithm for CBCT. We present an experiment where this technique is employed to create a dynamic iodine image in a software phantom. Proper tuning of the algorithm and comparison with alternative methods will be done in the near future. This approach also allows us to investigate additional regularizers, such as L1 sparsity or nuclear norm minimization. Furthermore, as the technique is an iterative reconstruction algorithm and hence computationally quite intensive, we can accelerate the algorithm by employing graphical processing units.

References

[1] D.C.Hansen and T. Sorensen, "Fast 4d cone-beam ct from 60 s acquisitions," *Phys. Im. in Rad. Oncology*, vol. 5, pp. 69–75, 2018.

[2] L. Ritschl, S. Sawall, M. Knaup, A. Hess, and M. Kachelriess, "Iterative 4d cardiac micro-ct image reconstruction using an adaptive spatio-temporal sparsity prior," *Phys. Med. Biol.*, vol. 57, pp. 1517–1525, 2012.

[3] A. Chambolle and T. Pock, "A first-order primal-dual algorithm for convex problems with applications to imaging," *Journal of Mathematical Imaging and Vision*, vol. 40, no. 1, pp. 120–145, May 2011.

[4] C. Mory and L. Jacques, "A modified 4d rooster method using the chambolle–pock algorithm," *Proc. 3rd Intl. Conf. on Image Formation in X-Ray CT*, pp. 191–193, 2014.
[5] O. Taubmann, V. Haase, G. Lauritsch, Y. Zheng, G. Krings, J. Hornegger, and A. Maier, "Assessing cardiac function from totalvariation- regularized 4d c-arm ct in the presence of angular undersampling," *Phys. Med. Biol.*, vol. 62, p. 2762–2777, 2017.
[6] V. Nikitin, M. Carlsson, F. Andersson, and R. Mokso, "Four-dimensional tomographic reconstruction by time domain decomposition," *IEEE Tran Comp. Im.*, pp. 1–1, Feb 2019.
[7] C. Cocosco, V. Kollokian, R.-S. Kwan, and A. Evans, "Brainweb: Online interface to a 3d mri simulated brain database," *NeuroImage*, vol. 5, no. 4, pp. part 2/4, S425, 1997.
[8] R. Karch, F. Neumann, M. Neumann, and W. Schreiner, "A three-dimensional model for arterial tree representation, generated by constrained constructive optimization," *Computers in Biology and Medicine*, vol. 29, no. 1, pp. 19 – 38, 1999.
[9] G. I. Taylor, "Dispersion of soluble matter in solvent flowing slowly through a tube," *Proc. Royal Soc. of London. Ser. A. Math. Phys. Sci.*, vol. 219, no. 1137, pp. 186–203, 1953.